

Analysis of Orientation Autocorrelation and Cross-Correlation Functions for Polyethylene in the Inclusion Complex with Perhydrotriphenylene

Türkan Haliloğlu and Wayne L. Mattice*

Institute of Polymer Science, The University of Akron, Akron, Ohio 44325-3909

Received September 29, 1992; Revised Manuscript Received March 10, 1993

ABSTRACT: The first and second orientation autocorrelation functions have been computed and analyzed for polyethylene in the inclusion complex with perhydrotriphenylene at 223, 300, and 373 K. Two coordinate systems have been used—an internal coordinate system defined by the polyethylene chain and an external coordinate system defined by the channel. The orientation autocorrelation functions are denoted by $M_{1,int}(t)$, $M_{2,int}(t)$, $M_{1,ext}(t)$, and $M_{2,ext}(t)$. Cross-correlation functions have also been computed. The trajectories that provide the raw data are those reported by Zhan and Mattice (*Macromolecules* 1992, 25, 4078) for *n*-tetracontane in a channel formed by 90 molecules of perhydrotriphenylene. The results show the dynamics of the internal and external motions occur on different time scales which can be conveniently separated. The rigid-body rotation about the chain axis dominates the overall chain motion. The short-term memory of the direction of this rotation produces a slight overshoot to the decay of $M_{1,ext}(t)$ and $M_{2,ext}(t)$ at 223 and 300 K. This feature can be rationalized by a simple model for the rigid-body rotation. The internal motions are of higher frequency. They are dominated by the librational motions of internal C-C bonds, on a picosecond time scale, within the *trans* rotational isomeric state.

Introduction

Recently we have used molecular dynamics simulations to study the conformation and mobility of poly(1,4-*trans*-butadiene),^{1,2} poly(1,4-*trans*-isoprene),³ and polyethylene^{4,5} in the channel of crystalline perhydrotriphenylene, poly(1,4-*trans*-butadiene) in the channel formed by a crystalline array of chains of the same polymer,^{2,6} and polyethylene in the channel of crystalline urea.⁷ Rapid motion, on a time scale of nanoseconds or faster, was detected in all systems, although in some cases, such as poly(1,4-*trans*-isoprene) in perhydrotriphenylene³ or poly(1,4-*trans*-butadiene) in the matrix of form I,² this motion is of limited amplitude. Other systems provide motion on a larger scale, when viewed from a polar coordinate system defined by the channel. In some cases, as in poly(1,4-*trans*-butadiene) in perhydrotriphenylene,^{1,2} transitions between discrete rotational isomeric states contribute to the motions, but in other cases, as in polyethylene in the same matrix,⁴ the rapid motion of the chain is achieved without the occurrence of rotational isomeric state transitions. The rapid motion observed in the molecular dynamics simulations of these two systems is consistent with the experimental detection of motion using NMR,^{8,9} as is the absence of such rapid motion for poly(1,4-*trans*-isoprene) in perhydrotriphenylene.¹⁰

In the case of polyethylene in perhydrotriphenylene, both experiment¹⁰ and simulation⁴ find the chain has an overwhelming preference for *trans* placements, but nevertheless the chain is extremely mobile in the channel. The activation energy for this rapid motion, as inferred from data collected over similar temperature ranges of 150 K, is 1.1 kcal mol⁻¹ as deduced by NMR¹⁰ and ~0.4 kcal mol⁻¹ as deduced from molecular dynamics trajectories.⁴ The very small values for the activation energy, coupled with the strong preference for *trans* placements and rapid motion, show the experiment and the simulation detect the same process.

Prior analysis of the molecule dynamics trajectories has shown contributions to the rapid motion from fluctuations in the torsion angles within *trans* placements at internal C-C bonds and from rigid-body rotation of the polyethylene about its long axis.⁴ The analysis has also shown

the rapid motion is not caused by random migration of a "twiston" along the chain.⁵

Here we seek a separation of the contributions from internal fluctuations in torsion angles and from rigid-body rotations. The procedure utilizes the traditional first and second orientation autocorrelation functions. The separation is achieved by the selection of the coordinate system in which the unit bond vectors are expressed. This analysis provides an improvement in the agreement between the activation energies determined by experiment and from simulation and provides a strong case for the importance of the rigid-body motion as being the primary contributor to this dynamics. We also characterize the extent of correlations in the internal fluctuations in torsion angles at bonds *i* and *i* + *j*.

Trajectories

The molecular dynamics trajectories are those described by Zhan and Mattice.⁴ They were computed using version 2.1 of CHARMM as provided by Polygen Corp. Waltham, MA.¹¹ The system contains a molecule of *n*-tetracontane, C₄₀H₈₂, in a channel consisting of 90 molecules of perhydrotriphenylene, C₁₈H₃₀, which are arranged in 6 stacks of 15 molecules each. The matrix has *a* = *b* = 14.125 ± 0.01 Å, *c* = 4.78 ± 0.01 Å, and *γ* = 120 ± 0.5°. The system of 90 molecules of perhydrotriphenylene and one molecule of *n*-tetracontane was represented by 4442 discrete atoms (1660 carbon atoms and 2782 hydrogen atoms). The simulations, each of duration 1 ns, were performed at 223, 300, or 373 K, using a time step of 0.5 fs for the integration. The coordinates were recorded at intervals of 10³ steps (0.5 ps) for subsequent analysis.

Orientation Autocorrelation Functions

The first and second bond autocorrelation and cross-correlation functions are usually defined for bonds *i* and *i* + *j* by

$$M_1(t) = \langle \mathbf{m}_i(0) \cdot \mathbf{m}_{i+j}(t) \rangle \quad (1)$$

$$M_2(t) = (1/2)\{3\langle [\mathbf{m}_i(0) \cdot \mathbf{m}_{i+j}(t)]^2 \rangle - 1\} \quad (2)$$

where $\mathbf{m}_i(0)$ and $\mathbf{m}_{i+j}(t)$ denote unit vectors rigidly attached to bond i at time 0 and to bond $i+j$ at time t , respectively. If $j = 0$, these equations yield the bond autocorrelations, and if $j \neq 0$, they yield cross-correlation functions. Angle brackets denote the statistical mechanical average.

Discussion of the dynamics of n -tetracontane in perhydrotriphenylene is facilitated by a slight elaboration of the usual notation. This elaboration is the addition of another subscript, either "int" or "ext", to $M_1(t)$ and $M_2(t)$. The subscript "int" denotes orientation autocorrelation functions calculated in a manner that prohibits any contribution from rotation of the molecule as a rigid body. An internal coordinate system is used for the computation of $M_{1,\text{int}}(t)$ and $M_{2,\text{int}}(t)$. They are determined completely by the fluctuations in torsion angles and bond angles. The subscript "ext" denotes orientation autocorrelation functions calculated using an external coordinate system. Rotation of the molecule as a rigid body contributes to $M_{1,\text{ext}}(t)$ and $M_{2,\text{ext}}(t)$ but not to $M_{1,\text{int}}(t)$ and $M_{2,\text{int}}(t)$. Fluctuations in torsion angles and bond angles contribute to all of the orientation autocorrelation functions.

The internal orientation autocorrelation functions were computed as follows: The coordinates of three consecutive bonded atoms, A_{i-2} , A_{i-1} , and A_i , define an internal coordinate system for bond i . As is the custom in applications of rotational isomeric state theory to single chains,¹² the X axis for bond i lies along the bond from A_{i-2} to A_i , the Y axis is in the plane of A_{i-2} , A_{i-1} , and A_i , with a positive projection on the bond from A_{i-2} to A_{i-1} , and the Z axis completes a right-handed coordinate system. The Y -axis for the coordinate system of bond 1 is defined using a hypothetical bond from a nonexistent atom, A_{-1} , to real atom A_0 , with the position of A_{-1} selected so there is a *trans* placement at bond 1. In any instantaneous conformation, the position vectors for all the atoms are expressed in the internal coordinate system for bond 1 by use of transformation matrices, T_i , formulated from the torsion angle and bond angle at bond i , and the bond vectors, \mathbf{l}_i , using standard methods.¹²

$$\mathbf{r}_{i,\text{int}} = \mathbf{l}_1 + T_1\mathbf{l}_2 + T_1T_2\mathbf{l}_3 + \dots + T_1T_2\dots T_{i-1}\mathbf{l}_i \quad (3)$$

A unit vector along bond i in this instantaneous conformation, expressed in the internal coordinate system of bond 1, is

$$\mathbf{m}_{i,\text{int}} = \frac{\mathbf{r}_{i,\text{int}} - \mathbf{r}_{i-1,\text{int}}}{l_i} \quad (4)$$

where l_i denotes the instantaneous length of bond i .

Each trajectory contains 2000 records of the position vector of each atom in the system, recorded at intervals of 0.5 ps. The $M_{1,\text{int}}(t)$ is computed from these records and eqs 3 and 4 as

$$M_{1,\text{int}}(t) = \frac{1}{n_b \tau_{\text{max}}} \sum_{i=1}^{n_b} \sum_{\tau=1}^{\tau_{\text{max}}} \mathbf{m}_{i,\text{int}}(\tau\Delta t) \cdot \mathbf{m}_{i+j,\text{int}}(\tau\Delta t+t) \quad (5)$$

Here n_b denotes the number of pairs of bonds i and $i+j$ in the system that are of the type for which $M_{1,\text{int}}(t)$ is being calculated. The time delay between the observation of $\mathbf{m}_{i,\text{int}}$ and $\mathbf{m}_{i+j,\text{int}}$ is denoted by t . The time interval between records in the trajectory file is denoted by Δt , which has the fixed value of 0.5 ps. The index τ can assume integer values in the range 0–2000, and thus $\tau\Delta t$ covers the range 0–1 ns, at intervals of 0.5 ps, thereby defining specific records in the trajectory file of length 1 ns. The upper range for τ , denoted by τ_{max} , is 2000 – $t/\Delta t$. Thus

the summation over i considers all possible pairs of bonds, and the summation over τ then considers all records in the trajectory file consistent with the selected values of i and t . The averaging required for $M_{2,\text{int}}(t)$ is accomplished with similar summations over i and τ .

$$M_{2,\text{int}}(t) = \frac{1}{2n_b \tau_{\text{max}}} \sum_{i=1}^{n_b} \sum_{\tau=1}^{\tau_{\text{max}}} \{3[\mathbf{m}_{i,\text{int}}(\tau\Delta t) \cdot \mathbf{m}_{i+j,\text{int}}(\tau\Delta t+t)]^2 - 1\} \quad (6)$$

If the only motion were the rotation of n -tetracontane as a rigid body, the chain would appear to be immobile (and the confining matrix would appear to move) when viewed from the perspective of the internal coordinate system for bond 1. Thus neither $M_{1,\text{int}}(t)$ nor $M_{2,\text{int}}(t)$ is affected by rigid-body rotation of n -tetracontane, because rigid-body rotation changes none of the terms in eq 3. On the other hand, internal motions of n -tetracontane that change T_i (such as fluctuations in bond angles, torsional oscillations within *trans* rotational isomeric states, and transition between rotational isomeric states) have an effect on $M_{1,\text{int}}(t)$ and $M_{2,\text{int}}$, through eq 3.

The use of an internal coordinate system defined by bonds 1 and 2 for assessment of the internal contributions to the overall dynamics, rather than a coordinate system defined by two other bonds, can be justified in the present case by two arguments. First, the magnitude of the fluctuations, $|\phi - \phi_{\text{trans}}|$, is nearly the same at all internal C—C bonds.⁴ At 300 K the value of $|\phi - \phi_{\text{trans}}|$ is about 9° at typical internal C—C bonds and increases to ~10° at the terminal C—C bonds. Hence, the end effect is small. Second, what small end effect there is will tend to overestimate the contribution to the overall dynamics, if the internal coordinate system is defined by bonds 1 and 2. As we shall see, even when evaluated in the coordinate system of bonds 1 and 2, we find that the internal motions are of lesser importance than the external motions. This conclusion would become stronger (but only mildly so) if the internal contribution were evaluated in an internal coordinate system defined by two bonds in the middle of the chain.

The external orientation autocorrelation functions were computed using coordinates of each atom as expressed in a right-handed coordinate system defined by the matrix of perhydrotriphenylene. This coordinate system is entirely independent of the internal conformation of n -tetracontane; indeed, it can be defined even when n -tetracontane is removed from the system. The Z axis of the external coordinate system is parallel to the axis of the channel (which is also the c axis of the ordered array of 90 molecules of perhydrotriphenylene). The Y axis is fixed at an arbitrarily chosen direction perpendicular to the Z axis, and the X axis completes the right-handed coordinate system. Each trajectory contains 2000 records of the position vector of each atom, $\mathbf{r}_{i,\text{ext}}$, of atom i in the external coordinate system, recorded at intervals of 0.5 ps. Unit vectors along each bond are obtained as

$$\mathbf{m}_{i,\text{ext}} = \frac{\mathbf{r}_{i,\text{ext}} - \mathbf{r}_{i-1,\text{ext}}}{l_i} \quad (7)$$

The averages required in eqs 1 and 2 are performed by taking both the position and time averages as

$$M_{1,\text{ext}}(t) = \frac{1}{n_b \tau_{\text{max}}} \sum_{i=1}^{n_b} \sum_{\tau=1}^{\tau_{\text{max}}} \mathbf{m}_{i,\text{ext}}(\tau\Delta t) \cdot \mathbf{m}_{i+j,\text{ext}}(\tau\Delta t+t) \quad (8)$$

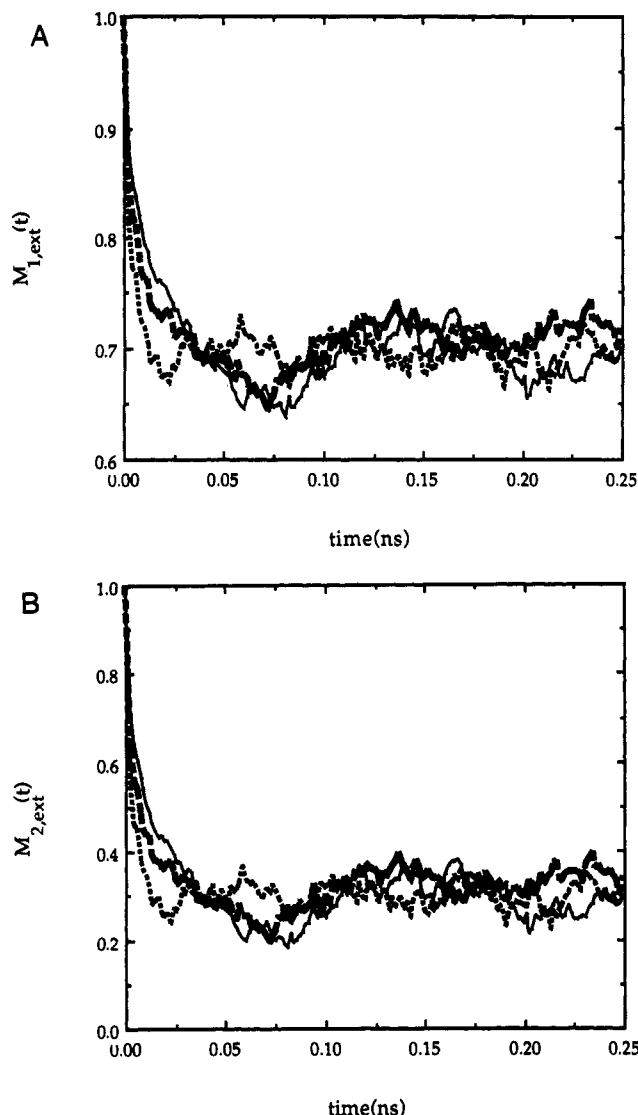


Figure 1. (A) First orientation autocorrelation function for C—C bonds in *n*-tetracontane at temperatures of 223 K (solid line), 300 K (long dashes), and 373 K (short dashes), computed using an external coordinate system defined by the channel. (B) Second orientation autocorrelation function for C—C bonds in *n*-tetracontane at temperatures of 223 K (solid line), 300 K (long dashes), and 373 K (short dashes), computed using an external coordinate system defined by the channel.

$$M_{2,\text{ext}}(t) = \frac{1}{2n_b \tau_{\text{max}}} \sum_{i=1}^{n_b} \sum_{\tau=1}^{\tau_{\text{max}}} \{3[\mathbf{m}_{i,\text{ext}}(\tau\Delta t) \cdot \mathbf{m}_{i+j,\text{ext}}(\tau\Delta t+t)]^2 - 1\} \quad (9)$$

Both $M_{1,\text{ext}}(t)$ and $M_{2,\text{ext}}(t)$ are affected by rotation of *n*-tetracontane as a rigid body and by internal fluctuations in bond angles and torsion angles.

Dynamics in an External Coordinate System

Appearance of the Autocorrelation and Cross-Correlation Functions. $M_{1,\text{ext}}(t)$ and $M_{2,\text{ext}}(t)$ for the C—C bonds in *n*-tetracontane at temperatures of 223, 300, and 373 K are depicted in parts A and B of Figure 1, respectively. The increase in mobility with increasing temperature causes the initial decay to become faster as the temperature increases, as expected. There is a slight overshoot in $M_{1,\text{ext}}(t)$ and $M_{2,\text{ext}}(t)$ at ~ 0.07 ns, which is more easily seen at the lower two temperatures. The limiting values at longer times are greater than zero due to the constraints on reorientation produced by the

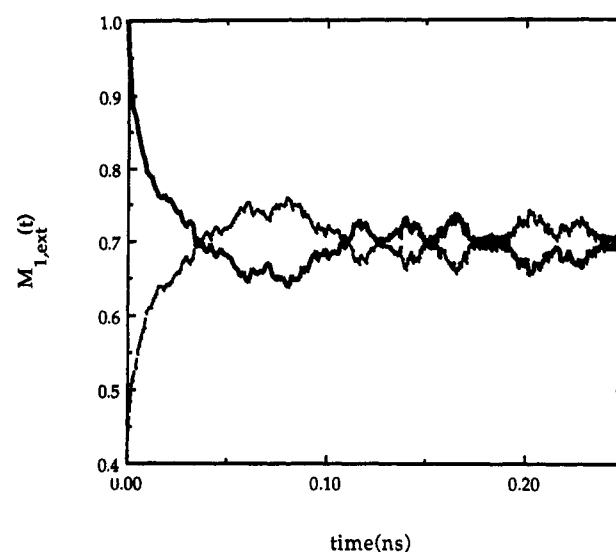


Figure 2. Autocorrelation function for C—C bonds (solid line) and cross-correlation function (dashed line) for nearest-neighbor C—C bonds in *n*-tetracontane at 223 K.

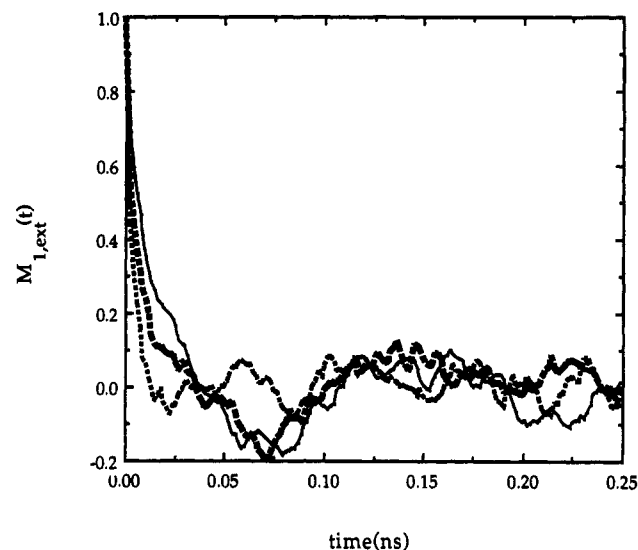


Figure 3. First orientation autocorrelation function for C—H bonds in *n*-tetracontane at 223 K (solid line), 300 K (long dashes), and 373 K (short dashes).

channel. The cross-correlation function for nearest-neighbor C—C bonds in *n*-tetracontane at 223 K is depicted in Figure 2, along with the autocorrelation function at the same *T* for comparison. These two $M_{1,\text{ext}}(t)$ start from different values, and the initial rapid changes are in opposite directions, but they both show the overshoot near ~ 0.07 ns and reach similar nonzero values at long times.

Orientation autocorrelation functions for the C—H bonds in *n*-tetracontane (Figure 3) decay to zero, in contrast with the autocorrelation and cross-correlation functions for the C—C bonds, but they retain the overshoot near ~ 0.07 ns at low temperatures. The rapid loss of correlation for the C—H bonds, which is evident in $M_{1,\text{ext}}(t)$ in Figure 3, is in agreement with the randomization of the orientation of the C—H bond about the long axis of the channel within 1 ns, as described earlier.⁴

Interpretation of the Autocorrelation and Cross-Correlation Functions. The behavior of the autocorrelation and cross-correlation functions can be interpreted with the aid of a very simple model depicted in Figure 4. The chain is viewed as a rigid body, with all bond angles and torsion angles frozen at the values adopted in the optimized *all-trans* conformation. The only motion

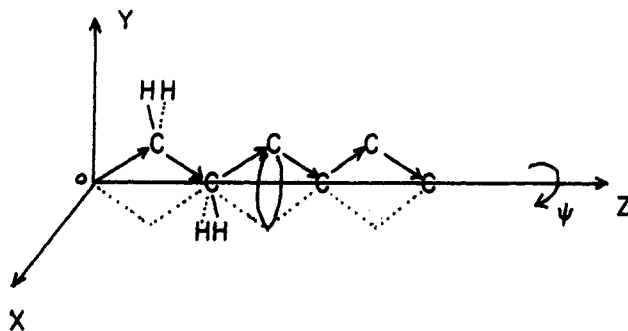


Figure 4. Sketch of a short polyethylene chain in the *all-trans* conformation in an external coordinate system, *OXYZ*, defined by the channel. The chain undergoes rigid-body rotation about the *Z* axis.

Table I. Times (ps) for $1/e$ of the Total Decay of the Autocorrelation Functions and the E_a Deduced from These Times

bond	223 K	300 K	373 K	E_a , kcal mol ⁻¹
C—C	10	7	4	1.0
C—H	10	6	4	0.95

accessible to the rigid body is rotation about its long axis, denoted by *Z* in Figure 4. This rotation is denoted by ψ , with $\psi > 0$ for clockwise rotation. Each C—C bond makes an angle of 34° (half of the supplement of $\angle C-C-C$) with the *Z* axis. The C—C bond vector sweeps out a cone as the rigid molecule passes through the entire range for ψ . Assuming all values of ψ become equally probable as $t \rightarrow \infty$ and the only motion is the one arising from rotation of the rigid body about the *Z* axis, the long-time limits for the orientation autocorrelation functions for the C—C bonds are predicted to be

$$\lim_{t \rightarrow \infty} M_{1,\text{ext}}(t) = 0.687 \quad (10)$$

$$\lim_{t \rightarrow \infty} M_{2,\text{ext}}(t) = 0.262 \quad (11)$$

This very simple model for the dynamics provides a nearly quantitative description of the limiting values for $M_{1,\text{ext}}(t)$ and $M_{2,\text{ext}}(t)$ in Figure 1. Since the C—H bonds in the same model must make an angle of 90° with the *Z* axis, the model predicts $M_{1,\text{ext}}(t)$ for these bonds will approach zero as $t \rightarrow \infty$, which is the result depicted in Figure 3. Furthermore, since the simple model assumes the chain rotates about the *Z* axis as a rigid body, the autocorrelation functions for the C—C and C—H bonds must have the same rate for their decay to their final values (and their temperature dependence must specify the same activation energy), although the final values of the autocorrelation functions themselves are different. This prediction of the simple model is well-approximated by the data, as shown in Table I. The activation energy obtained by this procedure, ~ 1 kcal mol⁻¹, is slightly larger than the one of ~ 0.4 kcal mol⁻¹ estimated from the temperature dependence of the average value of $d\langle\psi\rangle/dt$.⁴ It is in excellent agreement with the experimental result of 1.1 kcal mol⁻¹, obtained from the temperature dependence of the T_1 's.⁹

An explanation for the overshoot in the correlation functions as ~ 70 ps requires a slight elaboration of the simple model. Assume the value of ψ will always change by $|\Delta\psi|$ in the time interval δt , with δt chosen to be small enough so $|\Delta\psi| < \pi$. The assumption of a single value for $|\Delta\psi|$ is not correct, as we shall see momentarily, but its adoption is useful for generation of a simple rationalization of the overshoot. Let p denote the probability $\Delta\psi$ will have a positive sign in a time interval. Thus $p = 0$ or 1

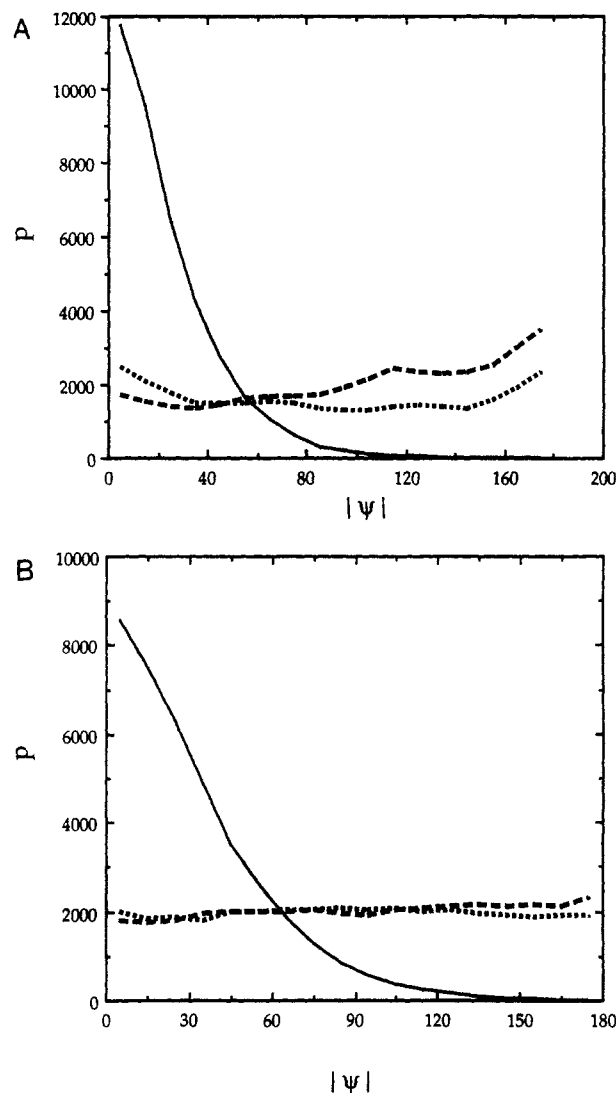


Figure 5. (A) Distribution of $|\psi|$ at 0.5 ps (solid line), 80.5 ps (long dashes), and 130.5 ps (short dashes) at 223 K. (B) Distribution of $|\psi|$ at 0.5 ps (solid line), 80.5 ps (long dashes), and 130.5 ps (short dashes) at 373 K.

implies continuous rotation of the chain in the same direction, with a constant angular velocity of absolute value $\Delta\psi/\delta t$. The correlation functions will be periodic, with period $2\pi\delta t/|\Delta\psi|$, if p is 0 or 1. In the case of the autocorrelation function of the C—C bonds, $M_{1,\text{ext}}(t)$ would oscillate between values of 1 and ~ 0.37 . Since the correlation functions depicted in Figures 1 and 2 are not periodic, neither of these limits for p is supported by the data. The actual correlation functions require $0 < p < 1$.

If $0 < p < 1$, the autocorrelation functions must eventually decay to a constant value. The decay may still contain an overshoot at short times if there is a residual short-term memory of the direction of the preceding rotation, due to rotational inertia, leading to an accumulation of an excess of chains that have rotated by $\sim 180^\circ$. The consequences of the short-term memory for the time dependence of the distribution for ψ are depicted in parts A and B of Figure 5. By definition, $\psi = 0$ when $t = 0$. The first observation at a later time, $t = 0.5$ ps, shows a distribution of $|\psi|$ because $\Delta\psi$ is not a constant in the real trajectory. (Strict adherence to the simple model would require a delta function at $|\psi| = \Delta\psi$ when $t = \delta t$.) The distribution is broader at the higher temperature. At 223 K, the distribution at 80.5 ps shows a slight excess at $|\psi| > \pi/2$, which produces the overshoot detected in the correlation functions depicted in Figures 1–3. A more

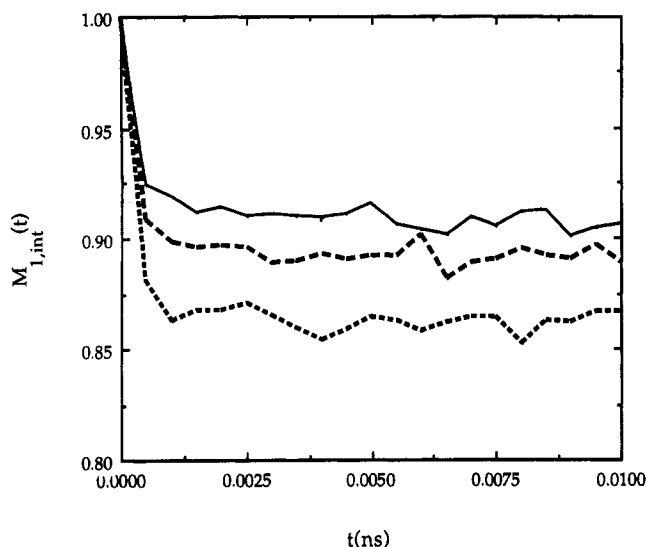


Figure 6. First orientation autocorrelation function for C—C bonds in *n*-tetracontane at temperatures of 223 K (solid line), 300 K (long dashes), and 373 K (short dashes), computed using an internal coordinate system.

nearly uniform distribution of $|\psi|$ is seen at 130.5 ps at 223 K. When the temperature is 373 K, the distribution of $|\psi|$ does not develop the excess at $|\psi| > \pi/2$, and there is no overshoot in the autocorrelation function, perhaps because of the broader distribution for $|\Delta\psi|$ at 373 K.

Dynamics in an Internal Coordinate System

Autocorrelation and Cross-Correlation Functions. Figure 6 depicts $M_{1,int}(t)$ for bond i at three temperatures. Nearly all of the decay has occurred within 10^{-3} ns, which is significantly faster than the decay of $M_{1,ext}(t)$ (Figure 1A). The rapid time scale of the decay in Figure 6 is consistent with the fast internal motion arising from fluctuations of torsion angles, ϕ , within the *trans* rotational isomeric states. It is not consistent with an origin in discrete rotational isomeric state transitions, $t \rightleftharpoons g$, which require a much longer time scale even when the chain moves in a less restrictive medium, such as a vacuum.¹³ The limiting values of $M_{1,int}(t)$ are temperature dependent, and they are always larger than the limit of ~ 0.7 which was obtained with the $M_{1,ext}(t)$ in Figure 1A. The decrease in $M_{1,int}(\infty)$ with increasing temperature arises from an increase in the amplitude of the torsional oscillations at higher temperature. The large values of $M_{1,int}(\infty)$ (compared to the values of ~ 0.7 for $M_{1,ext}(t)$ in Figure 1A) arise from the limited amount of randomization of the \mathbf{m}_i , which in turn is due to the small range of the torsional oscillations at all temperatures.

Since the decay of $M_{1,int}(t)$ is completed in 10^{-3} ns and only can produce a decay to $M_{1,int}(\infty) \sim 0.9$, we conclude the more important contribution to the overall disorder of the entire system, comprised of the polymer plus the matrix, is produced by the rigid-body rotation of the polymer about its long axis, which occurs on a somewhat longer time scale and yields a smaller $M_{1,ext}(\infty)$.

The autocorrelation functions depicted in Figure 6 were averaged over all C—C bonds in *n*-tetracontane. Previous measurements of the fluctuation in the torsion angle, $\delta\phi = (\langle\phi^2\rangle - \langle\phi\rangle^2)^{1/2}$, have shown these fluctuations are slightly larger for bonds at the end of the chain than for bonds in the middle of the chain. A dependence upon the position of the bond is also apparent in $M_{1,int}(t)$, as shown in Figure 7.

Figure 8 depicts several cross-correlation functions for C—C bonds i and $i + j$, $j = 0, 4, 10, 14, 18$. The influence

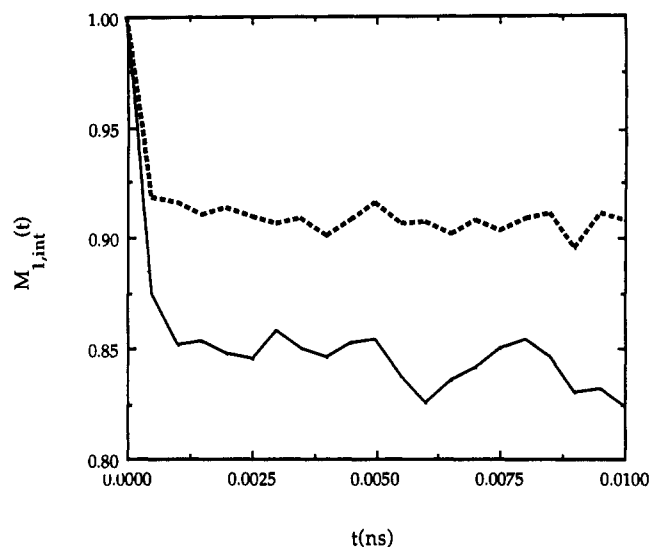


Figure 7. First orientation autocorrelation function at 223 K for the last C—C bond in the chain (solid line), compared with $M_{1,int}(t)$ for all C—C bonds (dashed line).

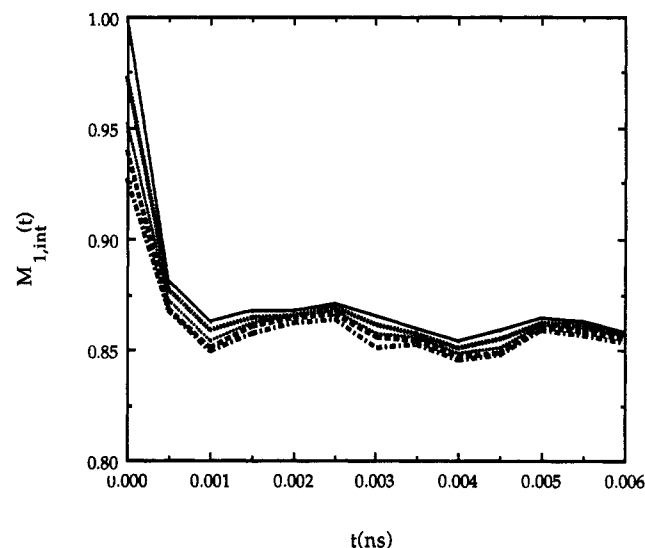


Figure 8. Cross-correlation functions, $M_{1,int}(t)$, for C—C bonds i and $i + j$ with $j = 0, 4, 10, 14, 18$, at 373 K, using the internal coordinate system.

of the channel is clearly present in the fact that these correlation functions do not differ greatly in shape. If the chain were free, the limiting values of $M_{1,int}(t)$ as $t \rightarrow \infty$ would decrease with increasing j and approach zero for $j = 18$. In the channel, the nature of the correlation of bonds i and $i + j$ is controlled primarily by whether j is odd or even (Figure 9), but it is nearly independent of the size of j otherwise.

Directions of Neighboring Bond Rotations. The Brownian dynamics simulations of a polyethylene-like chain have shown there is often a strong tendency of rotations of opposite sign at bonds i and $i + 2$ because these correlated motions reduce the displacement of the tails.¹⁴ One of the types of correlated rotational isomeric state transitions was $ttt \rightarrow g^+tg^-$. The *n*-tetracontane in the channel in perhydrotriphenylene cannot complete the $ttt \rightarrow g^+tg^-$ transition, because the environment is so confining that it will not permit occupancy of stable *gauche* states by the *n*-alkane. Although ϕ cannot make the changes of $\sim 120^\circ$ required for completion of a $t \rightarrow g$ rotational isomeric state transition, it is of interest to ascertain whether the fluctuations in ϕ , of magnitude much smaller than 120° , might be correlated such that they tend to be of opposite signs at bonds i and $i + 2$.

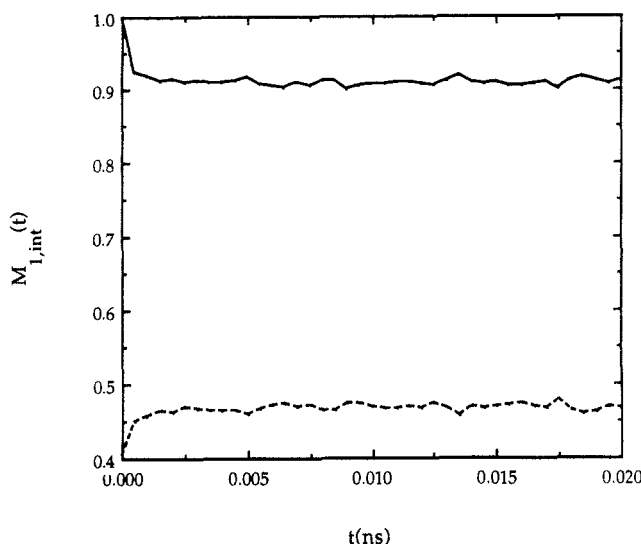


Figure 9. Cross-correlation functions, $M_{1,int}(t)$, for C—C bonds i and $i + j$, $j = 0$ and 1 , at 223 K, using the internal coordinate system.

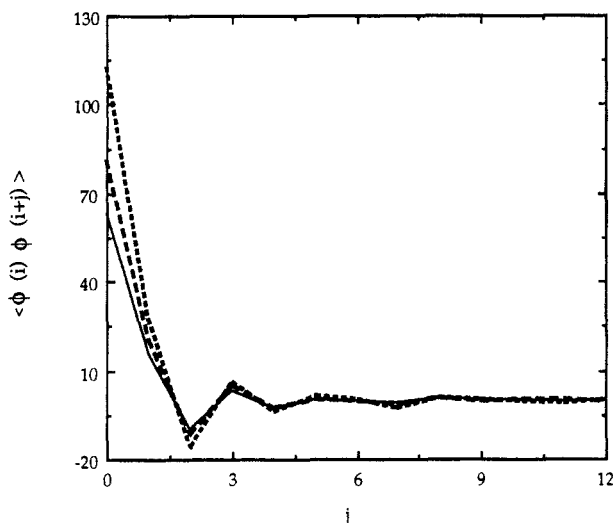


Figure 10. $\langle \phi_i \phi_{i+j} \rangle$, as a function of j , for n -tetracontane in perhydrotriphenylene at 223 K (solid line), 300 K (long dashes), and 373 K (short dashes). The zero for ϕ is at the *trans* placement.

Figure 10 depicts $\langle \phi_i \phi_{i+j} \rangle$ vs j , using the convention where $\phi = 0^\circ$ for a *trans* placement.

$$\langle \phi_i \phi_{i+j} \rangle = \frac{1}{n_b \tau_{\max}} \sum_{i=1}^{n_b} \sum_{\tau=1}^{\tau_{\max}} \phi_i \phi_{i+j} \quad (12)$$

When $j = 0$ the values increase with temperature due to the increase in the magnitude of the torsional oscillations in the *trans* state. Since the symmetry of the potential demands $\langle \phi \rangle = 0$, the sizes of the fluctuations, $\delta\phi$, are $\sim 7.9^\circ$, 9.0° , and 10.6° at 223, 300, and 373 K, respectively.

The values of $\langle \phi_i \phi_{i+j} \rangle$ alternate in sign for $j = 1-4$, being negative when j is even. The negative value at $j = 2$ shows there is indeed a tendency for torsions of opposite sign at bonds i and $i + 2$, as expected from the Brownian dynamics simulations. In the channel, however, the correlation between bonds i and $i + 1$, which tend to rotate in the same direction, is actually somewhat larger in magnitude than the correlation between bonds i and $i + 2$.

Conclusion

The mobility of n -tetracontane in the channel formed by perhydrotriphenylene has contributions from rotation as a rigid body about the c -axis of the channel and high-frequency torsional oscillations within the *trans* rotational isomeric states. These two types of motions occur on different time scales, which can be separated by orientation autocorrelation functions computed using internal and external coordinate systems. The rotation as a rigid body about the chain axis produces more disorder on the nanosecond time scale than do the oscillations of the internal degrees of freedom. The important features of the rigid-body rotation, namely, the temperature-independent limiting values of $M_{1,ext}(t)$ and $M_{2,ext}(t)$ and the tendency for an overshoot at low temperatures, can be rationalized with a simple model. The chain has a short-term memory of the sense, clockwise or counterclockwise, of its prior rotation. The fluctuations of the internal torsional angles tend to be correlated in the same sense for nearest-neighbor bonds and in the opposite sense for next-nearest-neighbor bonds. These internal fluctuations occur within *trans* states.

Acknowledgment. This research was supported by National Science Foundation Grant NSF DMR 89-15025.

References and Notes

- (1) Dodge, R.; Mattice, W. L. *Macromolecules* **1991**, *24*, 2709.
- (2) Zhan, Y.; Mattice, W. L. *Macromolecules* **1992**, *25*, 1554.
- (3) Zhan, Y.; Mattice, W. L. *Macromolecules* **1992**, *25*, 3439.
- (4) Zhan, Y.; Mattice, W. L. *Macromolecules* **1992**, *25*, 4078.
- (5) Zhan, Y.; Mattice, W. L. *Makromol. Chem., Macromol. Symp.*, in press.
- (6) Zhan, Y.; Mattice, W. L. *J. Chem. Phys.* **1992**, *96*, 3279.
- (7) Lee, K.-J.; Mattice, W. L.; Snyder, R. G. *J. Chem. Phys.* **1992**, *96*, 9138.
- (8) Sozzani, P.; Behling, R. W.; Schilling, F. C.; Brückner, S.; Helfand, E.; Bovey, F. A.; Jelinski, L. W. *Macromolecules* **1989**, *22*, 3318.
- (9) Schilling, F. C.; Sozzani, P.; Bovey, F. A. *Macromolecules* **1991**, *24*, 4369.
- (10) Sozzani, P.; Bovey, F. A.; Schilling, F. C. *Macromolecules* **1991**, *24*, 6764.
- (11) Brooks, B. R.; Brucoleri, R. E.; Olafson, B. D.; States, D. J.; Swaminathan, S.; Karplus, M. *J. Comput. Chem.* **1983**, *4*, 187.
- (12) Flory, P. J. *Macromolecules* **1974**, *7*, 381.
- (13) Zúñiga, I.; Bahar, I.; Dodge, R.; Mattice, W. L. *J. Chem. Phys.* **1991**, *95*, 5348.
- (14) Helfand, E.; Wasserman, Z. R.; Weber, A. *Macromolecules* **1980**, *13*, 526.